World Academy of Science, Engineering and Technology
International Journal of Computer and Information Engineering
Vol:16, No:5, 2022

Efficient Alias-free Level Crossing Sampling

Negar Riazifar, Nigel G. Stocks

Abstract—This paper proposes strategies in level crossing (LC) sampling and reconstruction that provide alias-free high-fidelity signal reconstruction for speech signals without exponentially increasing sample number with increasing bit-depth. We introduce methods in LC sampling that reduce the sampling rate close to the Nyquist frequency even for large bit-depth. The results indicate that larger variation in the sampling intervals leads to alias-free sampling scheme; this is achieved by either reducing the bit-depth or adding a jitter to the system for high bit-depths. In conjunction with windowing, the signal is reconstructed from the LC samples using an efficient Toeplitz reconstruction algorithm.

Keywords—Alias-free, level crossing sampling, spectrum, trigonometric polynomial

I. Introduction

MANY signals of physiological origin such as speech, ECG and EEG vary rapidly for brief moments and then remain constant for some time. Synchronous signal processing architectures do not take into account the temporal sparsity of these signals and, hence, classical uniform sampling in time can result in a large number of samples that convey little or no information. Level crossing (LC) analogue to digital converters (ADCs) [1], [2] have been shown to have significant benefits over conventional ADCs, not least they offer the potential of a significant reduction in operating power when signals are temporally sparse. In conventional LC (CLC) sampling, also known as sent-on-delta or implicit sampling [3], reference amplitude thresholds are regularly distributed along the amplitude range of the signal. A sample is triggered when the input signal $f(t)$ crosses one of these thresholds. If the times $t_1, t_2, \cdots$ are considered instants at which the amplitude levels are crossed, the sample pairs $\{t_j, f_j\}$ represent the signal, $f(t_j) = f_j$. Sampling time t_j depends only on the form of $f(t)$ and the threshold locations. The relationship between the bit-depth, B, and the number of thresholds, N, is $N = 2^B$.

In conventional ADC the input analogue signal is sampled uniformly in time [4]. This generates spectral replicas of signal energy at multiples of the sampling frequency. High-frequency noise would fold back to baseband if the input signal is not bandlimited to less than half of the sampling frequency. This is referred to aliasing which degrades the signal quality. Hence, there is considerable interest in LC ADCs due to the significant benefit of removing aliasing [5], [6].

To date, few studies have investigated the use of LC ADCs in the context of alias-free signal processing [7]–[9]. Tsividis [10] stated that since there is no sampling in time, no aliasing occurs. Wu [11] also stated that alias-free property of LC sampling is because the sampling rate adapts to the signal frequency. Whilst these studies claim that the spectrum is cleaner and has fewer distortion components at frequencies in the band of interest, no systematic quantitative analysis has been undertaken. Here we undertake such an analysis by investigating the impact of aliasing in a simulated LC ADC without an anti-aliasing filter.

Additionally, we propose strategies in LC sampling and reconstruction that not only provide high fidelity signal reconstruction for speech signals but also exploit the alias-free property to give highly efficient sampling protocols. The results indicate that the distribution of the intervals between samples highly affects signal reconstruction quality and also aliasing. The proposed sampling method improves the efficiency of the sampling by excluding samples that occur within a specified interval of the previous sample. The alias-free property enables a significant reduction in the number of samples whilst maintaining functionally useful signal quality.

There are different approaches of reconstruction from non-uniform sampling [12]. Many of these methods are numerically unstable due to ill-conditioning [13]. Here we reconstruct the signal based on trigonometric polynomials and an adaptive weights least square approach [14].

The objective of the paper is to develop LC sampling methods that yield alias-free property. By introducing a novel sampling method and using a trigonometric polynomial reconstruction method we show it is possible to reduce the sampling rate compared to CLC ADCs without significantly compromising the coding fidelity.

This paper is organised as follows. The reconstruction methodology is presented in Section II. Section III outlines the proposed sampling and reconstruction methodologies. The simulation and results for sinusoidal and speech signals are discussed in Sections IV and V. Lastly, Section VI concludes the paper.

II. Reconstruction from Irregular Samples

We consider the problem of reconstructing a band-limited function $f(t)$ from its set of irregular samples $\{f(t_j), j \in \mathbb{Z}\}$. We used adaptive-weight conjugate-gradient Toeplitz reconstruction method (ACT algorithm) [13]. We apply ACT algorithm to the oversampling problem; we oversample the signal by increasing the bit-depth to improve accuracy while negating the negative impact of exponentially increasing number of sample points.

An efficient and accurate approximation of $f(t)$ from data set $\{f(t_j), |t_j| \leq M\}$, $M > 0$ can be achieved by interpolating the data $f(t_j)$ using trigonometric polynomials [13], [14],

$$P_M = \{p : p(t) = \sum_{k=-M}^{M} a_M(k) \frac{e^{\frac{2\pi i k t}{2M+1}}}{\sqrt{2M+1}}, a_M(k) \in \mathbb{C} \quad (1)$$

N. Riazifar and N. G. Stocks are with the Department of Engineering, University of Warwick, Coventry, UK (e-mail: n.riazifar@warwick.ac.uk, n.g.stocks@warwick.ac.uk).

A unique trigonometric polynomial $p_M \in P_M$ of order M and period $2M+1$ fits the samples $f(t_j)$ in an interval $[-M, M]$. In order to avoid the boundary effects, the samples are taken in $J_M \subseteq [-M-1, M+1]$.

Suppose $\{t_j, f(t_j)\}, j \in \mathbb{Z}$ and $-M - \frac{1}{2} \leq t_1 < \cdots t_j < M + \frac{1}{2}$, is given and the sampling set satisfies the maximal gap condition (MGC) [13],

$$\sup(t_{j+1} - t_j) = \delta < \frac{1}{2f_{max}} = \frac{T_0}{2M}, j \in \mathbb{Z} \tag{2}$$

where δ is the largest interval in the whole sequence, T_0 is the record length, f_{max} is the maximum frequency in the trigonometric polynomial. Ideally, $p_M(t_j) = f(t_j)$. However, for finite M this is not equal, and the error should be minimized. The unique trigonometric polynomial, $p_M \in P_M$, solves least squares problem (LSP).

$$\sum_{j \in J_M} |p_M(t_j) - f(t_j)|^2 \frac{t_{j+1} - t_{j-1}}{2} = minimum \tag{3}$$

and $\lim_{M\to\infty} p_M(t) = f(t)$. LSP is an accurate reconstruction method for irregular sampling problem which can be solved by the inversion of a Toeplitz matrix [14]. C_M is considered the $(2M+1) \times (2M+1)$ positive Toeplitz matrix.

$$(C_M)_{kl} = \sum_{j \in J_M} \frac{w_j}{2M+1} e^{\frac{-2\pi i(k-l)t_j}{2M+1}}, |k|, |l| \leq M \tag{4}$$

where $w_j = \frac{t_{j+1} - t_{j-1}}{2} > 0, j \in \mathbb{Z}$, is a set of weights and only changes the amplitude of the components. They help to keep the condition number of a Toeplitz matrix low [13].

For a given sequence of LC samples $\{(t_j, f(t_j)), j \in J_M\}$ as an input, if condition $J_M \geq 2M+1$ is satisfied, $b_M \in \mathbb{C}^{2M+1}$ is computed as follows [14],

$$b_M(k) = \sum_{j \in J_M} f(t_j) \frac{w_j}{\sqrt{2M+1}} e^{\frac{-2\pi i k t_j}{2M+1}}, |k| \leq M \tag{5}$$

We can construct the trigonometric polynomial using (1). a_M is the matrix of Fourier coefficient and can be calculated by the inversion of C_M.

$$a_M = C_M^{-1} b_M \in \mathbb{C}^{2M+1} \tag{6}$$

ACT algorithm is a strong candidate for high-fidelity systems because adaptive weights improve ill-conditioning and hence numerical stability and exact reconstruction has been proven for band-limited signals [14].

III. Sampling and Reconstruction Methodologies

The accuracy of a LC ADC is governed by a number of factors that in practice are hardware dependent; generally, these relate to the accuracy of the samples and the method of reconstruction [15]. For this study, we assume that the thresholds and hence the samples t_j are known with infinite precision and the time quantization is arbitrarily accurate. With these assumptions, the reconstruction method becomes the limiting factor in determining the SNR of the ADC [16] and hence the fundamental limit of this method can be evaluated.

A notable advantage of employing an adaptive-weights Toeplitz formalism is that the numerical conditioning is theoretical well established [13]. The condition number of the Toeplitz matrix has been obtained,

$$cond\, C_M \leq \left(\frac{1 + 2\delta M}{1 - 2\delta M}\right)^2 \tag{7}$$

It is notable that the conditioning of the problem is governed entirely by the maximal gap δ and the order of the polynomial M. Reducing δ (e.g. by increasing B) clearly improves the condition number and may be expected therefore to enhance the accuracy of the reconstruction. In CLC sampling large gaps between samples can occur naturally and the MGC may be violated. Such a situation is expected to lead to numerical instability. Our proposed sampling algorithm aims to achieve the benefits of oversampling by increasing bit-depth but to avoid the exponential increase in the number of samples.

First, we introduce what we term the reduced CLC (RCLC) algorithm to exploit redundancy in the parts of the signal that are over represented. The CLC sampling gives a set of sample pairs $\{t'_j, f'_j\}$. For high bit-depth the set $\{t'_j, f'_j\}$ is large and reconstruction is computationally expensive. We therefore remove samples that are 'close together'. Sample t'_{j+1} is removed if $\Delta'_j < T_{min} = C * T_N = C * \frac{1}{2BW}$, $\forall \Delta'_j$, where $\Delta'_j = t'_{j+1} - t'_j$, T_{min} is the minimum temporal difference between samples, T_N is the inverse of the Nyquist frequency, BW is the bandwidth of the original signal and $C > 0$ is a coefficient that enables control over T_{min}. This procedure leads to a reduced LC sample set with new sample pairs $\{t''_j, f''_j\}$ with a new time interval $\Delta''_j = t''_{j+1} - t''_j$.

Removing samples might violate MGC. We, therefore, propose an interpolation approach to reduce δ. New samples are inserted if $\Delta''_j > T_{max} = \frac{T_0}{2M}$, where we introduce T_{max} as the maximum temporal difference between samples. First order interpolation between adjacent samples $\{t''_j, f''_j\}$ and $\{t''_{j+1}, f''_{j+1}\}$ is employed to get the final LC pairs $\{t_j, f_j\}$ used to reconstruct the original signal. We term this algorithm RCLC sampling with interpolation or RCLCI. One significant benefit of RCLCI is that we can save the RCLC instead of RCLCI data set since we can do the interpolation as a part of the digital to analogue converter (DAC); This makes the proposed sampling method very efficient.

IV. Simulation

Simulations were carried out in MATLAB using a speech signal sourced from the TIMIT database [17]. The signal was upsampled from the original 16kHz to 10MHz to enable highly accurate approximation of the LC samples. However, it does not affect the cost because in practice the algorithms are designed for continuous time signals and no upsampling is required. The oversampled signal was partitioned into 50% overlapping frames, W_k [12] each of duration $T_0 = 10$ms. W_k is called capture frame. We designate the central sub-frame within W_k as a separate frame, $w_k \subset W_k$, and call it the evaluation frame. w_k is of length $\frac{T_0}{2}$. The partitioning of these

frames is illustrated in Fig. 1. We apply a Hamming window to reduce end effects followed by the RCLCI sampling algorithm before reconstructing the signal using the ACT method on each capture frame. To further reduce end effects $\frac{1}{4}$ of each capture frame is discarded. The frames are then concatenated to reconstruct the whole signal. Accuracy of signal reconstruction is expressed using SNR between the original signal $f(t)$ and the reconstruction $p_M(t)$,

$$SNR = 10\log\frac{\sum_n f^2[n]}{\sum_n \left(f[n] - p_M[n]\right)^2} \tag{8}$$

where $p_M[n] = p_M(t = nT)$.

V. Results

A. RCLC and RCLCI Sampling

Fig. 2 illustrates SNR Vs M using CLC and RCLC samples. Clearly the SNR is dependent on the choice of M. As M increases the fitted polynomial captures higher frequency content and hence the SNR initially improves; but for large M numerical instability occurs, particularly at low bit-depth, because the MGC in (2) becomes violated. Transition to unstable reconstruction is observed approximately at values of $M = 50$, 90 for $B = 8$, 10 respectively.

The RCLC algorithm aims to improve the energy efficiency of the sampling process by reducing the number of samples acquired. For $B = 8$, 10, 15, the CLC sampling method generates 1306, 5224, 167004 samples respectively; while RCLC reduces the number of samples to 323, 421, 522. This comparison shows high redundancy in the CLC samples. The same SNR is observed in both cases despite the removal of samples by the RCLC sampling scheme; e.g. for $B = 15$ the RCLC algorithm removes more than 99% of the samples and yet the maximal SNR is unchanged. This observation implies that in the design of LC ADCs the performance is strongly affected by the distribution of the time intervals between samples.

Fig. 3 demonstrates the number of intervals that violate MGC in the RCLC sampling algorithm. It is observed for approximately zero intervals violating the MGC, e.g. $B = 15$, the SNR is maximised (Fig. 2). For $B = 8$, 10 where we have a reasonable number of violations the SNR is reduced. This observation clearly shows when MGC is not met there is no guarantee the trigonometric polynomial is a good approximation [14]. One is therefore led to conclude that the number of large intervals does impact adversely on the reconstruction accuracy; numerical stability governs the accuracy.

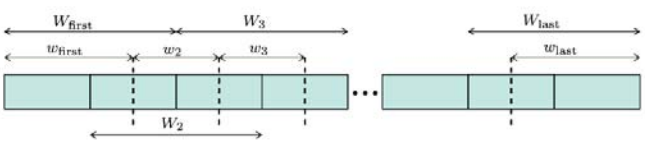

Fig. 1 Partitioning of signal into capture frames W_k and evaluation frames w_k, adapted from [12]

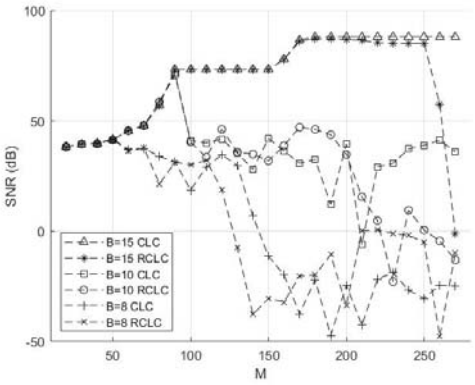

Fig. 2 SNR Vs M using CLC and RCLC sampling methods on a windowed time speech frame for $C = 0.3$ and $B = 8$, 10, 15

Another interesting observation is that the SNR does not depend directly on the bit-depth i.e. increasing bit-depth does not necessarily lead to an increase in the SNR. In regions of stable reconstruction, the SNR is the same for all bit-depths and only depends on the value of M used in the reconstruction [18]. For example, for $M \leq 50$ the number of violations of MGC for $B = 8$, 10, 15 is near 0. Although some of the intervals violate the MGC, it is still numerically stable. However, increasing bit-depth reduces the maximum gap size δ thus enabling stable reconstruction at higher values of M. These observations lead to a practical recommendation for the choice of M. The largest value of M for which the MGC is satisfied gives the maximum SNR; hence $M = \frac{T_0}{2\delta}$.

Although increasing M improves the SNR, ultimately numerical instability limits the maximum value of M that can be used. When the MGC is violated the instability occurs; this significantly affects the signal reconstruction quality. In principle, using a high bit-depth to decrease δ can reduce numerical instability. However, since the value of δ depends also on the statistics of the signal this approach cannot guarantee success. We, therefore, use the RCLCI sampling algorithm to satisfy MGC.

Fig. 4 shows how varying coefficient C impacts SNR and the number of samples in the RCLCI method. The dashed line

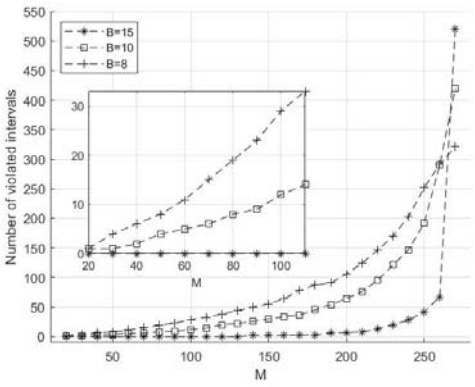

Fig. 3 Number of intervals that violate MGC in RCLC method on a windowed time speech frame for $C = 0.3$ and $B = 8$, 10, 15

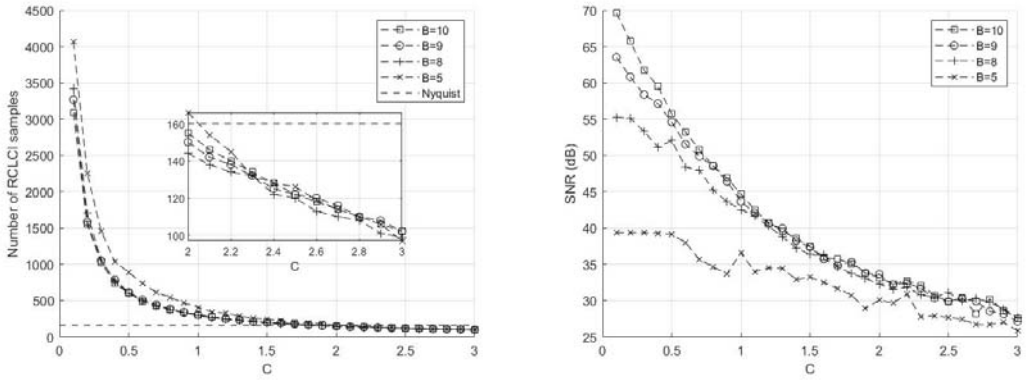

(a) (b)

Fig. 4 (a) Number of RCLCI samples and (b) SNR of RCLCI samples Vs C on a windowed time speech frame for $B = 5$, 8, 9, 10 and $M = \frac{T_0}{2CT_N}$

shows the number of samples that are required to satisfy the Nyquist criteria under conditions of uniform sampling. The input bandwidth of the signal is 8kHz and a sampling rate of 16KHz leads to 160 samples in a 10ms time window. C determines T_{min} and hence controls the redundancy between samples. $C = 1$ corresponds, approximately, to a sampling rate that just satisfies Nyquist criteria. The value of M that optimises the SNR is approximated when $T_{max} = T_{min}$. This condition can be used to calculate the optimal value as $M = \frac{T_0}{2CT_N}$. For each value of C, the optimal value of M is used to reconstruct the signal. It can be observed that $C < 1$ provides more data points, because it reduces the minimum time interval T_{min}, and yields high SNR. However, if C is increased beyond the Nyquist sampling interval, reasonable reconstruction can still be achieved. For instance, for $C = 2$, the points are rejected at twice the Nyquist rate, $M = 40$ and $B = 10$, RCLCI generates only 155 points, while SNR is as high as 33 dB. Because interpolation helps to prevent numerical instability. Fig. 4 demonstrates a good choice of C provides coding efficiency and also a good SNR reconstruction.

We also note that the RCLCI algorithm enhances SNR at low bit-depths and the erratic variation in SNR due to numerical instability no longer exists. For instance, the comparison of Fig. 4 and Fig. 2 demonstrates for $C = 0.3$, $B = 8$ and using the optimal value $M = 260$, the RCLCI technique delivers approximately 53 dB; whilst the numerical instability is observed in CLC and RCLC techniques.

B. Aliasing Effect on Sinusoidal Signal

The RCLC and RCLCI algorithms aim to remove aliasing effect. We consider this analysis in this section for an asymptotically generated periodic signal. Preliminary investigations of aliasing effect using the proposed RCLCI sampling and reconstruction methods were carried out in MATLAB on a 12 harmonic sinusoidal input signal, each harmonic at 1kHz separation, with 100Hz frequency resolution.

To see the impact of aliasing we start from a position where we have high SNR. We picked $C = 0.5$ to have at least 240 samples to ensure the MGC is satisfied and we can resolve the bandwidth; This should give a high SNR starting point. The aliasing is then introduced by increasing the bandwidth of the signal through adding extra frequency component beyond 12kHz. We define it as 'out-of-band frequency component'. The impact of weak out-of-band signals can be more accurately assessed by choosing sampling parameters that minimise spectral leakage and hence yield a very low noise floor. An out-of-band high frequency component was added at 36kHz with an amplitude specified as a fraction of the root mean square (RMS) of the signal.

The impact of aliasing can be assessed by looking at the spectrum of the fitted Fourier coefficients a_M. Fig. 5 demonstrates the spectrum of the original signal and the Fourier coefficients without introducing out-of-band component for $M = 120$ and $B = 10$. Clearly 24 sharp spikes with a noise floor of -290dB is observed. The remarkably small background indicates there is no spectral leakage and, hence, we have effectively achieved robust reconstruction.

We define 'an alias component' as a narrowband peak in the in-band spectrum below the Nyquist frequency due to the

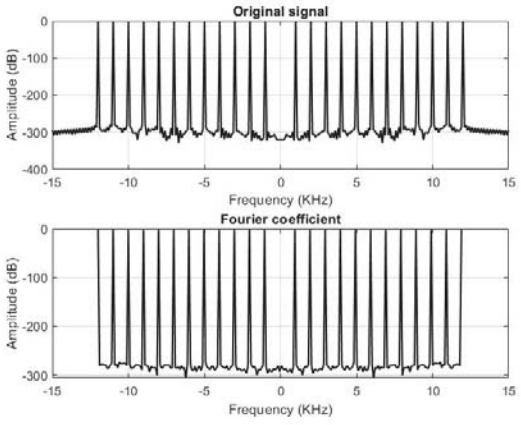

Fig. 5 Spectrum of the original signal and the Fourier coefficients of reconstructed signal using RCLCI sampling method on a 12 harmonic sinusoidal signal for $C = 0.5$, $M = 120$ and $B = 10$

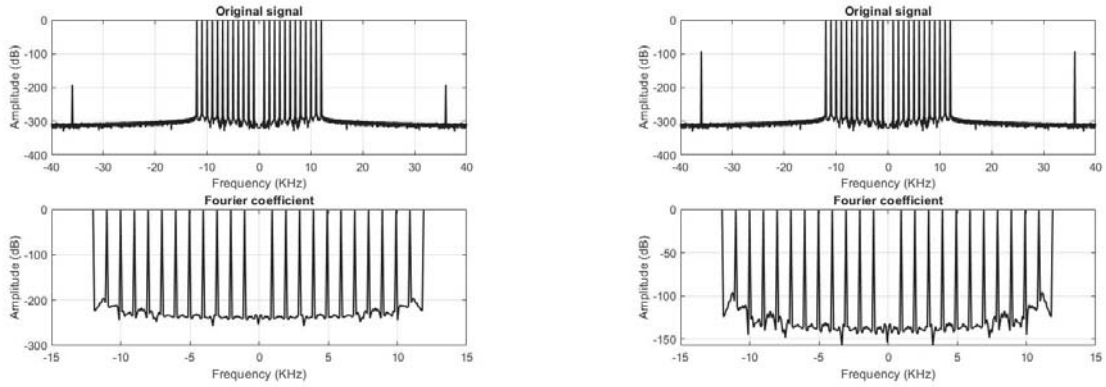

(a) (b)

Fig. 6 Spectrum of the original signal and the Fourier coefficients of reconstructed signal using RCLCI sampling method on a 12 harmonic sinusoidal signal for $C = 0.5$, $M = 120$ and $B = 10$ when the amplitude of the out-of-band frequency component, is (a) -192.21 dB and (b) -92.21 dB

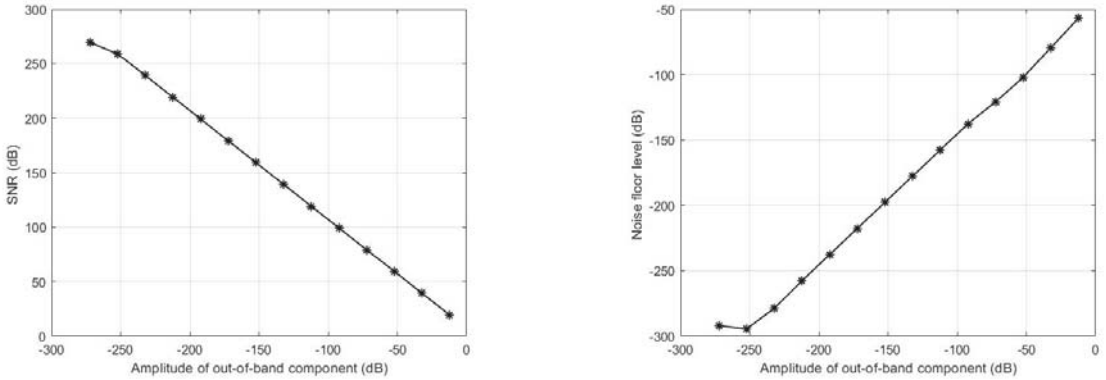

(a) (b)

Fig. 7 (a) SNR and (b) noise floor Vs amplitude of the out-of-band frequency component using RCLCI sampling method on a 12 harmonic sinusoidal signal for $C = 0.5$, $M = 120$ and $B = 10$

out-of-band frequency component.

Fig. 6 compares the Fourier coefficient spectrum for two different amplitude of the out-of-band frequency component, -192.21 dB and -92.21 dB. It is notable that aliasing does not occur to happen in a single point in the frequency domain. The energy of the aliased component is still in the spectrum but not at a particular component. This energy is being spread to other regions; It is being whitened. Hence, the system is alias-free but with an increased noise floor. We define 'aliasing noise floor' as a noise floor generated by the out-of-band harmonic component; The power in the out-of-band component is converted to white noise and added to the spectral background of baseband. The system is classified as 'alias-free' when there is no alias component even though the noise background increases. We note that the aliasing noise floor is approximately 60dB and 160dB higher than the background in the original spectrum in panels (a) and (b) respectively.

The impact of aliasing can be measured systematically. Fig. 7 demonstrates how SNR (panel (a)) and the spectral background level (panel (b)) changes as a function of the amplitude of the out-of-band frequency component. As expected, reducing the amplitude achieves higher SNRs. Furthermore, Fig. 7(b) clearly demonstrates that the out-of-band frequency component is effectively being whitened, turned into noise and added as an aliasing noise floor. Indeed, if we set the amplitude of this out-of-band component to 0, this noise floor would also drop down to -300dB.

It is also necessary to understand the relationship between the power in the out-of-band frequency component and the power in the aliasing noise floor. Fig. 8 compares these two powers. The power of the signal is expressed as sum of the absolute squares of its time domain samples divided by the signal length,

$$P_x = \lim_{N\to\infty} \frac{1}{2N+1} \sum_{n=-N}^{N} |x[n]|^2 \tag{9}$$

It is notable that the power of the out-of-band component is almost identical to the additional power in spectral background. This observation further supports the proposition that the energy in the out-of-band peak is now distributed across the whole spectrum; There is almost an exact correspondence between the increase in the size of the noise floor and the amplitude of the out-of-band component.

It is of some interest to compare the RCLCI method to standard ADC theory. We therefore now consider a standard uniform sampling method (Fig. 9). We introduced an out-of-band frequency component at 37kHz and uniformly sampled the same 12 harmonic sinusoidal input signal using the same sampling frequency as the RCLC sampling rate. As expected, an alias component is observed at the folding frequency, at 10.1kHz, in Fig. 9; Clearly due to the spectral leakage smaller amplitude of an alias component is observed. One is therefore led to conclude that the observed alias-free phenomena occurs because of the RCLCI sampling approach and not because of the ACT reconstruction method.

C. Aliasing Effect on Speech Signal

In this section we investigate the impact of aliasing using the speech signal. We took the TIMIT signal and added a single out-of-band frequency component at 25kHz, which is well beyond the bandwidth of the signal, 8kHz. Fig. 10 demonstrates the spectrum of this original signal when the amplitude of the out-of-band component is 10% of the signal's RMS.

The comparison of the Fourier coefficients of the reconstructed signal using RCLC, RCLCI and standard uniform sampling methods and ACT reconstruction technique for $C = 0.5$, $M = 130$ and $B = 7$ is also illustrated in Fig. 11. The top and middle panels indicate RCLC and RCLCI sampling is alias-free in a sense that power in the out-of-band component is not reflected back to a single peak; it is added to the total noise background. Since the amplitude of the out-of-band component is 10% of the signal's RMS, 10th of the energy is redistributed in the reconstructed spectrum across all frequencies. However, an alias component is clearly observed using standard uniform sampling method (Bottom panel). We uniformly sampled the signal using the same sampling frequency as the RCLCI sampling rate. Indeed one expects a single alias component to be observed at the folding frequency, at 9.3kHz. This observation is consistent with the results in the previous section for the sinusoidal input signal.

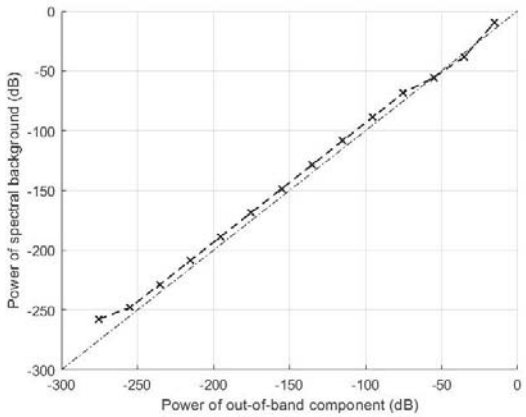

Fig. 8 Comparison of power in the out-of-band frequency component and the power in the aliasing noise floor using RCLCI sampling method on a 12 harmonic sinusoidal signal for $C = 0.5$, $M = 120$ and $B = 10$

Fig. 12 monitors the effect of changing the amplitude of the out-of-band frequency component on SNR and aliasing noise floor for $C = 0.5$ and $M = 130$. We chose $B = 6$ since this provides alias-free behaviour using RCLC and RCLCI sampling methods and hence, aliasing noise floor level can clearly be investigated. According to panel (a), the SNR is strongly affected by the choice of amplitude. As expected, smaller amplitudes achieve higher SNRs. It can also be observed that the SNR plateaus as the amplitude is reduced. This is perhaps not surprising because the signal with tiny amplitude variation, due to the out-of-band high frequency component, is likely to cross the thresholds for lower bit-depths. This leads to no further information for signal reconstruction and, hence, the SNR plateaus. However, similar behaviour as Fig. 7(a) is observed for higher bit-depths ($B \geq 10$).

Fig. 12(b) compares the power in the out-of-band frequency component and the power in the aliasing noise floor. Noise floor is achieved by the subtraction of two sets of Fourier coefficient spectrum with and without out-of-band component. The difference in amplitude quantifies the increased power in the spectral background due to the presence of out-of-band high frequency component; Higher amplitude, higher level of aliasing noise floor. This figure suggests that there is a broadband additive white noise in spectrum.

Fig. 13 illustrates the spectrum of the fitted Fourier coefficients for a fixed amplitude, -61.53 dB, and frequency, 25kHz, of the out-of-band component and for $B = 6, 7, 10, 11, 14, 15$. The comparison of the spectrum for $B = 6, 7$ and the original spectrum (Fig. 10) demonstrates that RCLCI sampling method is alias-free for $B = 6$ and almost $B = 7$ because there is no sharp peak as an alias component. Furthermore, the spectral background level is increased by approximately 10 dB for frequencies between 10kHz and 13kHz. The aliasing noise floor is introduced by being added to the broadband background.

In principle, for lower bit-depths, fewer of samples would be close to T_{min} in the rejection step (RCLC) and, therefore, the time interval between samples is more randomised. Whilst for higher bit-depths, larger number of samples fall very close to T_{min}; This increases correlation between the points and hence makes the sample set more uniform and uniformity gives rise to sharp alias component.

It is observed in Fig. 13 that as the bit-depth goes up, the alias component is getting sharper whilst the background noise is reduced. For instance, comparing $B = 10$ and 15 shows that the amplitude of the alias component is increased by 2.23 dB for $B = 15$ but the level of the spectral background is reduced by approximately 10 dB for frequencies between 10kHz and 13kHz. This figure is a beautiful illustration of how we change the bit-depth and hence make the signal more uniform and we go from alias-free situation, $B = 6$, where the background is larger than fully alias scenario, $B = 15$, where we have strong alias component but the random background is reduced.

Another interesting observation is that according to Table I, SNR is approximately identical for all bit-depths; i.e., increasing bit-depth does not necessarily lead to improve the performance. In regions of stable reconstruction, the SNR

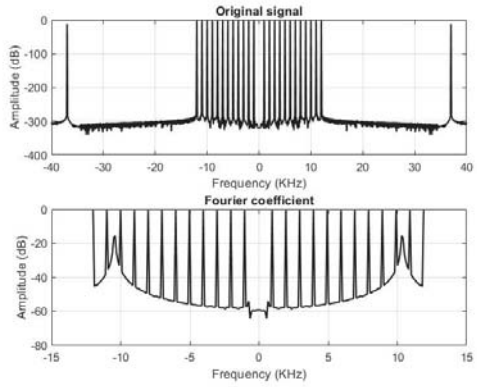

(a)

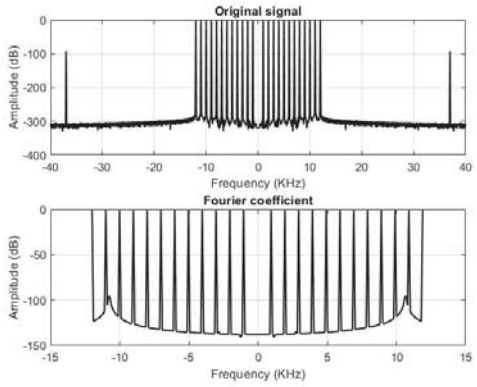

(b)

Fig. 9 Spectrum of the original signal and the Fourier coefficients of reconstructed signal using RCLCI sampling method on a 12 harmonic sinusoidal signal for $C = 0.5$, $M = 120$ and $B = 10$ when the amplitude of the out-of-band frequency component is (a) -12.21 dB and (b) -92.21 dB

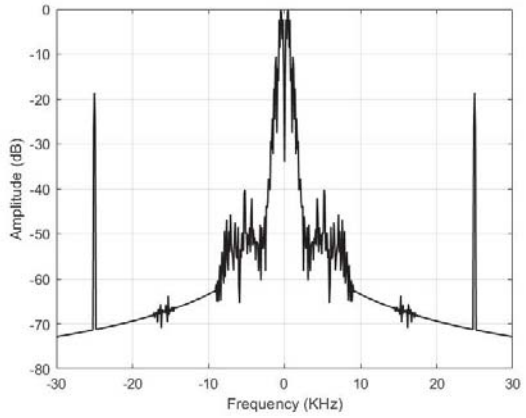

Fig. 10 Spectrum of the original signal using RCLCI sampling method on a windowed time speech frame for $C = 0.5$, $M = 130$ and $B = 7$

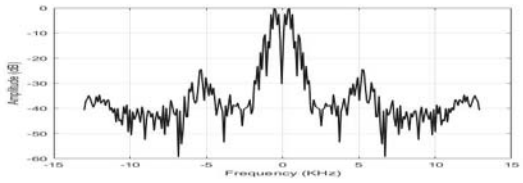

(a)

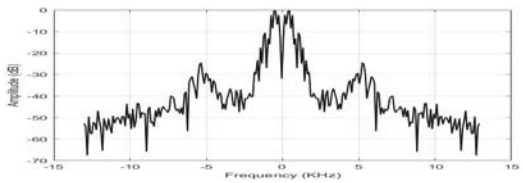

(b)

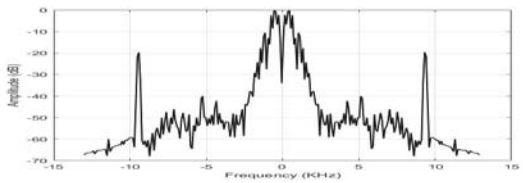

(c)

Fig. 11 Spectrum of the Fourier coefficients of reconstructed signal using (a) RCLC, (b) RCLCI and (c) uniform sampling methods on a windowed time speech frame for $C = 0.5$, $M = 130$ and $B = 7$

only depends on the value of M used in the reconstruction [18]. This observation suggests that RCLCI stabilises the reconstruction at lower bit-depths and also benefits from no aliasing property.

The presence of an alias component for high bit-depths due to increased uniformity of the distribution can be diminished by introducing jitter to T_{min}; We have effectively a jittered sampling scheme. Adding jitter makes the RCLCI sample set more randomised. The statistic of the jitter in our system is the statistics of the signal itself crossing the thresholds whereas in a standard jittered system the statistics of the added noise can be controlled.

Fig. 14 illustrates the spectrum of the Fourier coefficients and Table II shows the SNR and the number of samples when applying jitter for the same amplitude and frequency of the out-of-band component as Fig. 13 and $B = 6, 7, 10, 11, 14, 15$. Clearly, introducing jitter and hence increasing the randomness of the time intervals between samples will reduce the aliasing effect and broaden sharp peak of alias component, particularly for high bit-depths without any effect on SNR. Indeed, the out-of-band frequency component is converted from harmonic distortion to white noise. This is consistent with the known results in literature [9], [19]. One is therefore led to conclude that the randomness of sample intervals has a strong bearing on alias-free behaviour.

TABLE I
SNR AND THE NUMBER OF SAMPLES USING RCLCI SAMPLING METHODS ON A WINDOWED TIME SPEECH FRAME FOR $C = 0.5$, $M = 130$ AND $B = 6, 7, 10, 11, 14, 15$

B	6	7	10	11	14	15
SNR(dB)	21.51	21.47	21.38	21.37	21.38	21.37
# sample	409	343	322	318	321	321

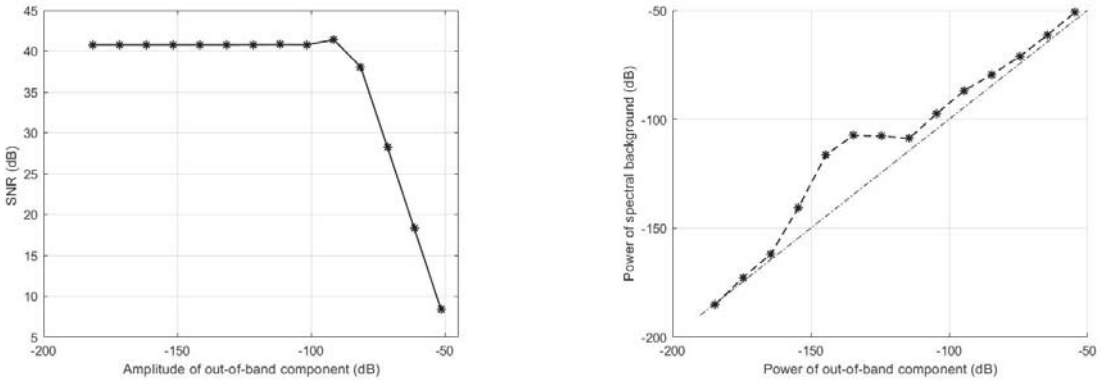

(a) (b)

Fig. 12 (a) SNR Vs amplitude of the out-of-band frequency component and (b) power in the aliasing noise floor Vs power in the out-of-band frequency component using RCLCI sampling method on a windowed time speech frame for $C = 0.5$, $M = 130$ and $B = 6$

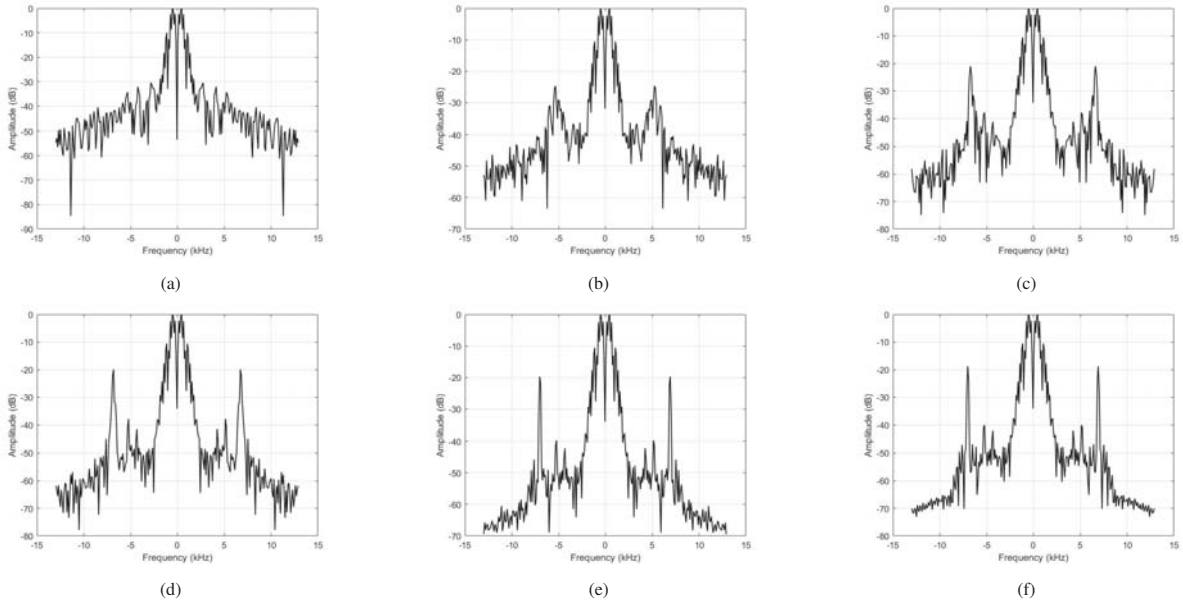

(a) (b) (c)

(d) (e) (f)

Fig. 13 Spectrum of the Fourier coefficients of reconstructed signal using RCLCI sampling method on a windowed time speech frame for $C = 0.5$, $M = 130$ and (a) $B = 6$, (b) $B = 7$, (c) $B = 10$, (d) $B = 11$, (e) $B = 14$ and (f) $B = 15$

VI. Conclusion

New sampling methods in conjunction with ACT reconstruction algorithm are observed to facilitate alias-free signal reconstruction. These efficient methods exploit redundancy between samples and enhance the numerical stability. The results also demonstrate that whitening of the aliased components reduces the effective bit-depth of the LC ADC but beneficially results in highly efficient coding. Hardware implementations would benefit from low bandwidth requirements (reduced sampling rates) and require no anti-aliasing filters.

TABLE II
SNR and the Number of Samples Using RCLCI Sampling Methods on a Windowed Time Speech Frame When Applying Jitter for $C = 0.5$, $M = 130$ and $B = 6, 7, 10, 11, 14, 15$.

B	6	7	10	11	14	15
SNR(dB)	21.55	21.62	21.28	21.15	21.53	21.48
# sample	399	362	327	322	324	320

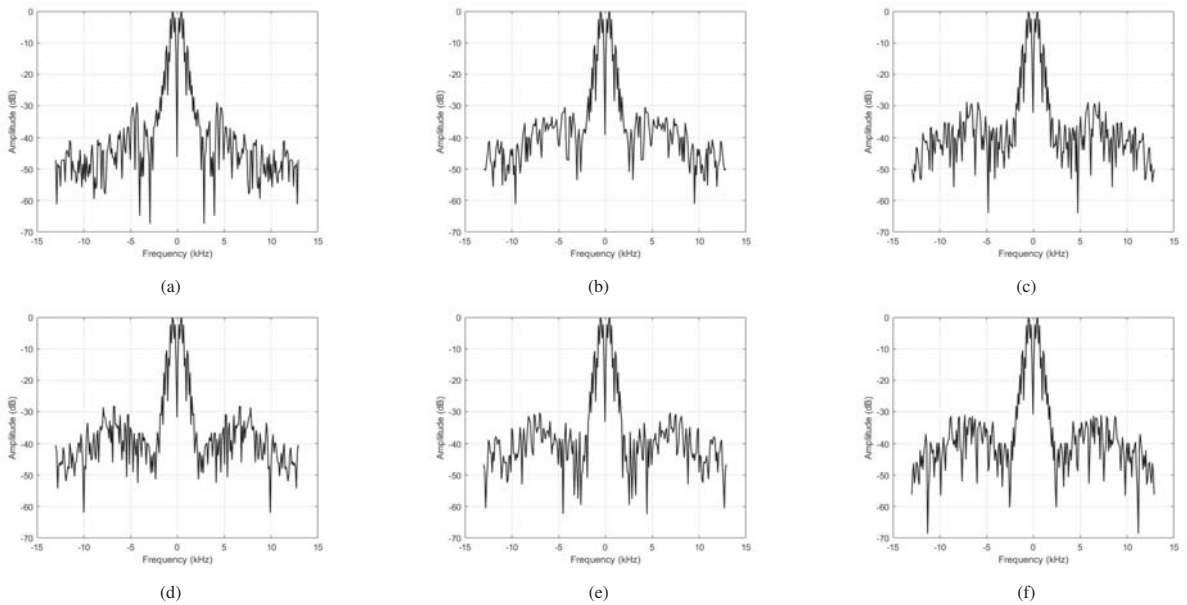

Fig. 14 Spectrum of the Fourier coefficients of reconstructed signal using RCLCI sampling method on a windowed time speech frame when applying jitter for $C = 0.5$, $M = 130$ and (a) $B = 6$, (b) $B = 7$, (c) $B = 10$, (d) $B = 11$, (e) $B = 14$ and (f) $B = 15$

REFERENCES

[1] E. Allier, G. Sicard, L. Fesquet and M. Renaudin, "Asynchronous level crossing analog to digital converters," *Meas. J. Int. Meas. Confed.*, vol. 37, pp. 296–309, 2005.

[2] N. Sayiner, H. V. Sorensen and T. R. Viswanathan, "A level-crossing sampling scheme for A/D conversion," *IEEE Transaction on Circuits and Systems-11: Analog and Digital Signal Processing*, vol. 43, pp. 335-339, 1996.

[3] D. Rzepka, M. Miśkowicz, D. Koscielnik and N. T. Thao, "Reconstruction of signals from level-crossing samples using implicit information," *IEEE Access*, vol. 6, pp. 35001–35011, 2018.

[4] D. Hand and M. S. W. Chen, "A non-uniform sampling ADC architecture with embedded alias-free asynchronous filter," *GLOBECOM - Signal Process. Commun. Symp.*, pp. 3707–3712, 2012.

[5] B. Schell and Y. Tsividis, "A continuous-time ADC/DSP/DAC system with no clock and with activity-dependent power dissipation," *IEEE J. Solid-State Circuits*, vol. 43, pp. 2472–2481, 2008.

[6] T. F. Wu, S. Dey and M. S. W. Chen, "A nonuniform sampling ADC architecture with reconfigurable digital anti-aliasing filter," *IEEE Trans. Circuits Syst. I Regul. Pap.*, vol. 63, pp. 1639–1651, 2016.

[7] S. Patil, A. Ratiu, D. Morche and Y. Tsividis, "A 3–10 fJ/conv-step error-shaping alias-free continuous-time ADC," *IEEE Journal of Solid-State Circuits*, vol. 51, pp. 908–918, 2016.

[8] M. Kurchuk, C. W. Wu, D. Morche and Y. Tsividis, "Event-driven GHz-range continuous-time digital signal processor with activity-dependent power dissipation," *IEEE Journal of Solid-State Circuits*, vol. 47, pp. 2164-2173, 2012.

[9] C. Luo, "Non-uniform sampling: algorithms and architectures," PhD Thesis, Georgia Institute of Technology, 2012.

[10] Y. Tsividis, "Digital signal processing in continuous time: A possibility for avoiding aliasing and reducing quantization error ," *IEEE International Conference on Acoustics, Speech, and Signal Processing*, vol. 2, pp. 589-592, 2004.

[11] T. F. Wu, C. R. Ho and M. S. W. Chen, "A flash-based non-uniform sampling ADC with hybrid quantization enabling digital anti-aliasing filter," *IEEE J. Solid-State Circuits*, vol. 52, pp. 2335–2349, 2017.

[12] C. Wijenayake, J. Scutts and A. Ignjatović, "Signal recovery algorithm for 2-level amplitude sampling using chromatic signal approximations," *Signal Processing*, vol. 153, pp. 143–152, 2018.

[13] H. G. Feichtinger, K. Grochenig and T. Strohmer, "Efficent numerical methods in non-uniform sampling theory," *Numer. Math.*, vol. 69, pp. 423-440, 1995.

[14] K. Grochenig, "Irregular sampling, Toeplitz matrices, and the approximation of entire functions of exponential type," *Math. Comput.*, vol. 68, pp. 749-765, 2002.

[15] K. Kozmin, J. Johansson and J. Delsing, "Level-crossing ADC performance evaluation toward ultrasound application," *IEEE Trans. Circuits Syst. I Regul. Pap.*, vol. 56, pp. 1708–1719, 2009.

[16] M. B. Mashhadi, N. Salarieh, E. S. Farahani and F. Marvasti, "Level crossing speech sampling and its sparsity promoting reconstruction using an iterative method with adaptive thresholding," *IET Signal Process.*, vol. 11, pp. 721–726, 2017.

[17] J. S. Garofolo, L. F. Lamel, W. M. Fisher, J. G. Fiscus, D. S. Pallett, N. L. Dahlgren and V. Zue, "TIMIT acoustic-phonetic continuous speech corpus," 1993. URL: https://catalog.ldc.upenn.edu/LDC93S1.

[18] N. Riazifar and N. G. Stocks, "Efficient high fidelity signal reconstruction based on level crossing sampling," *World Academy of Science, Engineering and Technology*, vol. 5, pp. 487-496, 2021.

[19] I. Bilinskis, E. Boole and K. Sudars, "Combination of periodic and alias-free non-uniform signal sampling for wideband signal digitizing and compressed transmitting based on picosecond-resolution event timing," *Signal Processing Symposium*, 2017.